

# Obtaining efficient collisional engines via velocity dependent drivings

Iago N. Mamede, Angel L. L. Stable and C. E. Fiore<sup>1</sup>

<sup>1</sup>*Universidade de São Paulo, Instituto de Física, Rua do Matão, 1371, 05508-090 São Paulo, SP, Brazil*  
(Dated: September 5, 2022)

Brownian particles interacting sequentially with distinct temperatures and driving forces at each stroke have been tackled as a reliable alternative for the construction of engine setups. However they can behave very inefficiently depending on the driving used for the worksource and/or when temperatures of each stage are very different from each other. Inspired by some models for molecular motors and recent experimental studies, a coupling between driving and velocities is introduced as an alternative ingredient for enhancing the system performance. Here, the role of this new ingredient for leveraging the engine performance is detailed investigated from stochastic thermodynamics. Exact expressions for quantities and distinct maximization routes have been obtained and investigated. The search of an optimal coupling provides a substantial increase of engine performance (mainly efficiency), even for large  $\Delta T$ . A simple and general argument for the optimal coupling can be estimated, irrespective the driving and other model details.

## I. INTRODUCTION

One of the main goals of nonequilibrium thermodynamics is to understand, from an operational point of view, the conversion between distinct amounts of energy delivered and those converted into useful power output [1]. Such fundamental issue appears in several systems in nature, encompassing physical [2–5], biological [6, 7], chemical processes [8], quantum technologies and others, thereby illustrating the great deal of attention for describing thermal machines operating at the nanoscale [2, 3]. Among the setups, we cite those composed of quantum-dots [9], colloidal particles [4, 5, 10], single [11] and coupled systems [12, 13] acting as working substance and others [14]. Most of above examples deal with engines operating under fixed or time-periodic variation of external parameters.

Collisional machines has also been tackled as a candidate for reliable thermal engines, in which the system is sequentially exposed to a distinct thermal reservoir and external driving forces and the time required for switching the thermal baths at the end of each stage being neglected. Despite its reliability in distinct situations, encompassing systems interacting only with a small fraction of the environment and those presenting distinct drivings over each member of system [15–18], such class of systems can operate inefficiently depending on the way it is projected (temperatures, kind of driving and duration of each stroke). For this reason, recent strategies, such an optimal switching time between thermal baths [19, 20] and the choice of an appropriate driving [21] at each stroke have been proposed and investigated. However about improvements can be limited when heat can not be converted into output work and the temperature difference  $\Delta T$  between strokes increases, yielding small efficiencies [20–22].

Aimed at circumventing above limitation, we introduce a new ingredient as an strategy for improving the efficiency of thermal engines. It consists of including a velocity dependent driving resulting in the generation of output power due to two component drivings: the first, given by  $f_i h_i(t)$ , coming from an arbitrary driving  $h_i(t)$  with strength  $f_i$ , whereas the second, given by  $\alpha f_i v_i$ , accounts to the coupling between the driving strength and velocity  $v_i$ , where parameter  $\alpha$  quanti-

fies its weight. Driving forces proportional to the velocity are rarely explored theoretically [23, 24], but they are present in distinct experimental studies such as, an electrical force stemming from delayed feedback [25], self-motile colloidal particles [26], catalytic nanomotors [27] and others [28].

This paper is organized as follows: Sec. II presents the main equations, system thermodynamics and distinct optimization routes. Results and phase diagrams are presented in Sec. III and conclusions are drawn in Sec. IV.

## II. THERMODYNAMICS OF COLLISIONAL ENGINES

One of the simplest engines is composed of a Brownian particle with mass  $m$  sequentially placed in contact with a given thermal reservoir and subjected to an external force  $\tilde{f}_i(t)$  at each stage. Each contact has a duration of  $\tau/N$  (with  $\tau$  and  $N$  being the total time and the number of strokes, respectively) and occurs during the intervals  $\tau_{i-1} \leq t < \tau_i$ , where  $\tau_i = i\tau/N$  for  $i = 1, \dots, N$ , in which the particle evolves in time according to the following Langevin equation

$$\frac{dv_i}{dt} = -\gamma_i v_i + \tilde{f}_i(t) + \xi_i(t), \quad (1)$$

where quantities  $v_i$ ,  $\gamma_i$  and  $\tilde{f}_i(t)$  denote its velocity, the viscous constant and the driving force respectively. As stated previously,  $\tilde{f}_i(t)$  is given by the time dependent driving plus a velocity dependent components  $\tilde{f}_i(t) = (h_i(t) - \alpha v_i) f_i$ , where  $\alpha$  is a constant. Note that one recovers the standard collisional engine as  $\alpha = 0$  [20, 22]. The interaction between particle and the  $i$ -th environment is described by the white-noise stochastic force  $\xi_i(t)$ , satisfying the white-noise properties:

$$\langle \xi_i(t) \rangle = 0 \quad , \quad \langle \xi_i(t) \xi_i(t') \rangle = 2\gamma_i T_i \delta_{ii'} \delta(t - t'), \quad (2)$$

where  $T_i$  is the bath temperature. In order to obtain the thermodynamics, let  $P_i(v, t)$  the velocity probability distribution with time evolution described by the Fokker-Planck (FP) equation [29–32]:

$$\frac{\partial P_i}{\partial t} = -f_i h_i(t) \frac{\partial P_i}{\partial v} - \frac{\partial J_i}{\partial v_i}, \quad (3)$$

where  $J_i$  is given by

$$J_i = -\beta_i v_i P_i - \gamma_i T_i \frac{\partial P_i}{\partial v_i}, \quad (4)$$

and  $\beta_i = \gamma_i + \alpha f_i$ . Note that the term  $\alpha f_i$  can be incorporated with  $\gamma_i v_i$  and can be viewed as a new quantity to be optimized, together the external force  $f_i$ . For simplifying matters, from now on, we shall assume  $k_b = m = 1$ .

From the FP equation and by performing the usual boundary conditions in the space of velocities, in which both  $P_i(v, t)$  and  $J_i(v, t)$  vanish as  $|v| \rightarrow \infty$ , the first and second law of thermodynamics can be derived. Starting with the former, the time variation of the energy system  $U_i = \langle E_i \rangle$  is given by  $dU_i/dt = -(\dot{W}_i + \dot{Q}_i)$ , where  $\dot{W}_i(t)$  and  $\dot{Q}_i(t)$  denote the work per unity of time (power) and heat flux from the system to the environment (thermal bath) reading

$$\dot{W}_i(t) = -f_i \langle v_i \rangle(t) \quad \text{and} \quad \dot{Q}_i(t) = \beta_i \langle v_i^2 \rangle(t) - \gamma_i T_i, \quad (5)$$

respectively. Analogously, time evolution of entropy  $S_i(t) = -\langle \ln[P_i(v_i, t)] \rangle$  is given by

$$\frac{dS_i}{dt} = \frac{1}{\gamma_i T_i} \left[ \int \frac{J_i^2}{P_i} dv_i + \beta_i \int v_i J_i dv_i \right], \quad (6)$$

where the first and second right terms are identified as the entropy production rate  $\Pi_i(t)$  and entropy flux  $-\Phi_i(t)$ , respectively [30–32]. The entropy flux can be rewritten in a more convenient way:

$$\Phi_i(t) = \frac{\beta_i}{\gamma_i T_i} [\beta_i \langle v_i^2 \rangle(t) - \gamma_i T_i]. \quad (7)$$

Summarizing, above expressions for thermodynamic quantities can be calculated from ensemble averages  $\langle v_i \rangle(t)$  and  $\langle v_i^2 \rangle(t) = b_i(t) + \langle v_i \rangle^2(t)$ . Since the coupling between velocity and external driving can be incorporated into Eq. (4), the probability distribution has a similar form to the couplingless case [22] and presents a Gaussian form:

$$P_i(v, t) = \frac{1}{\sqrt{2\pi b_i(t)}} \exp\left\{-\frac{1}{2b_i(t)} [v - \langle v_i \rangle(t)]^2\right\}, \quad (8)$$

in which the mean  $\langle v_i \rangle(t)$  and variance  $b_i(t) = \langle v_i^2 \rangle(t) - \langle v_i \rangle^2(t)$  are time dependent and obey the following equations

$$\frac{d\langle v_i \rangle(t)}{dt} = -\beta_i \langle v_i \rangle(t) + f_i h_i(t) \quad (9)$$

and

$$\frac{db_i(t)}{dt} = -2\beta_i b_i(t) + 2\gamma_i T_i, \quad (10)$$

respectively. Continuity of  $P_i(v, t)$  at each stroke implies that  $\langle v_i \rangle(\tau_i) = \langle v_{i+1} \rangle(\tau_i)$  and  $b_i(\tau_i) = b_{i+1}(\tau_i)$  (for all  $i = 1, \dots, N$ ), respectively. Since the system returns to the initial state after a complete period,  $\langle v_1 \rangle(0) = \langle v_N \rangle(\tau)$  and  $b_1(0) = b_N(\tau)$ , all averages  $\langle v_i \rangle(t)$ 's and variances can be solely calculated in terms of model parameters, that is, from the driving, temperature reservoirs, coupling  $\alpha$  and the period. By focusing on the simplest design of an engine composed of only two strokes and returning to the initial step after one cycles, expressions for averages and variances can be obtained for an arbitrary driving:

$$\langle v_1 \rangle(t) = e^{-\beta_1 t} \left( f_1 \mathcal{F}_1(t, \alpha) + \frac{f_2 e^{\frac{\beta_1 \tau}{2}} \mathcal{F}_2(\tau, \alpha) + f_1 \mathcal{F}_1\left(\frac{\tau}{2}, \alpha\right)}{e^{\frac{1}{2}(\beta_1 + \beta_2)\tau} - 1} \right), \quad (11)$$

and

$$\langle v_2 \rangle(t) = e^{-\beta_2(t - \frac{\tau}{2})} \left( f_2 \mathcal{F}_2(t, \alpha) + \frac{f_1 e^{\frac{\beta_2 \tau}{2}} \mathcal{F}_1\left(\frac{\tau}{2}, \alpha\right) + f_2 \mathcal{F}_2(\tau, \alpha)}{e^{\frac{1}{2}(\beta_1 + \beta_2)\tau} - 1} \right), \quad (12)$$

for the mean velocities and

$$b_1(t) = \frac{\gamma(e^{\beta_2 \tau} - 1)(\beta_1 T_2 - \beta_2 T_1) e^{\beta_1 \tau - 2\beta_1 t}}{\beta_1 \beta_2 (e^{(\beta_1 + \beta_2)\tau} - 1)} + \frac{\gamma T_1}{\beta_1}, \quad (13)$$

and

$$b_2(t) = \frac{\gamma(e^{\beta_1 \tau} - 1)(\beta_2 T_1 - \beta_1 T_2) e^{\beta_2 \tau - 2\beta_2(t - \frac{\tau}{2})}}{\beta_1 \beta_2 (e^{(\beta_1 + \beta_2)\tau} - 1)} + \frac{\gamma T_2}{\beta_2}, \quad (14)$$

for variances, respectively, where  $\mathcal{F}_1(t, \alpha) = \int_0^t e^{\beta_1 t'} h_1(t') dt'$  and  $\mathcal{F}_2(t, \alpha) = \int_{\tau/2}^t e^{\beta_2(t' - \frac{\tau}{2})} h_2(t' - \frac{\tau}{2}) dt'$ . From above expressions, all thermodynamic quantities are straightforwardly evaluated. Starting with the work (actually the power), averaged over a complete period, it follows that:

$$\overline{\dot{W}}_1 = -\frac{f_1}{\tau} \int_0^{\frac{\tau}{2}} h_1(t) e^{-(\gamma + \alpha f_1)t} \left( f_1 \mathcal{F}_1(t, \alpha) + \frac{f_2 e^{\frac{(\gamma + \alpha f_1)\tau}{2}} \mathcal{F}_2(\tau, \alpha) + f_1 \mathcal{F}_1\left(\frac{\tau}{2}, \alpha\right)}{e^{\frac{1}{2}[2\gamma + (f_1 + f_2)\alpha]\tau} - 1} \right) dt \quad (15)$$

and

$$\overline{\dot{W}}_2 = -\frac{f_2}{\tau} \int_{\frac{\tau}{2}}^{\tau} h_2(t) e^{-(\gamma + \alpha f_2)(t - \frac{\tau}{2})} \left( f_2 \mathcal{F}_2(t, \alpha) + \frac{f_1 e^{\frac{(\gamma + \alpha f_2)\tau}{2}} \mathcal{F}_1\left(\frac{\tau}{2}, \alpha\right) + f_2 \mathcal{F}_2(\tau, \alpha)}{e^{\frac{1}{2}[2\gamma + (f_1 + f_2)\alpha]\tau} - 1} \right) dt, \quad (16)$$

respectively, where they were expressed in terms of forces strengths. Note that  $\bar{W}_i$ 's are general and valid for all components  $h_i(t)$ 's. In contrast to collisional engines with no velocity dependent component ( $\alpha = 0$ ) [20, 22], they do not present a quadratic dependence on forces  $f_1$  and  $f_2$ , but reduces to them in such a limit.

Analogously, having expressions for  $\langle v_1^2 \rangle(t)$  and  $\langle v_2^2 \rangle(t)$ , averages  $\bar{Q}_1$  ( $\bar{Q}_2$ ) can be calculated and decomposed as a sum of two terms:  $\bar{Q}_1 = \bar{Q}_{1f} + \bar{Q}_{f_1, f_2, T_1}$  ( $\bar{Q}_2 = \bar{Q}_{2f} + \bar{Q}_{f_1, f_2, T_2}$ ), the former term given by  $\bar{Q}_{1f} = \int_0^{\tau/2} \langle v_1 \rangle^2(t) dt / \tau$  ( $\bar{Q}_{2f} = \int_{\tau/2}^{\tau} \langle v_2 \rangle^2(t) dt / \tau$ ) and accounting to the contribution for heat due to drivings, whereas the latter  $\bar{Q}_{f_1, f_2, T_1}$  reads  $\bar{Q}_{f_1, f_2, T_1} = \int_0^{\tau/2} b_1(t) dt / \tau - \frac{\gamma T_1}{2}$ , and describes the interplay between strength forces  $f_i$ 's, temperatures of reservoirs  $T_i$ 's and  $\alpha$ . From expressions for  $b_i(t)$ 's, each above component is given by:

$$\bar{Q}_{f_1, f_2, T_1} = \frac{(e^{(1+\alpha f_1)\tau} - 1)(e^{(1+\alpha f_2)\tau} - 1)[\alpha(f_1 T_2 - f_2 T_1) + T_2 - T_1]}{2\tau(e^{\tau(\alpha(f_1+f_2)+2)} - 1)(1 + \alpha f_1)(1 + \alpha f_2)}, \quad (17)$$

and  $\bar{Q}_{f_1, f_2, T_1} = -\bar{Q}_{f_1, f_2, T_2}$ . Note that their values averaged over a full period implies that  $\bar{Q}_1 + \bar{Q}_2 + \bar{W}_1 + \bar{W}_2 = 0$ , in consistency with the first law of thermodynamics. Finally, having  $\bar{Q}_i$ 's, the the steady entropy production is promptly obtained from Eq. (7) and given by  $\bar{Q}_1/T_1 + \bar{Q}_2/T_2$ .

### A. Constant and linear drivings

In order to compare such new ingredient with collisional engines [20–22], analysis will be exemplified for the two simplest kinds of drivings: constant and linear ones. Both of them have strengths  $f_1$  and  $f_2$ , the former being time independent with at  $0 < t \leq \tau/2$  and  $\tau/2 < t \leq \tau$ , respectively, whereas the latter is given by

$$h_i(t) = \begin{cases} \gamma t; & 0 \leq t < \tau/2 \\ \gamma(t - \tau/2); & \tau/2 \leq t < \tau \end{cases} \quad (18)$$

Thermodynamic quantities are directly evaluated from Eqs. (16)-(17).

### B. Efficiency

In several cases, the entropy production assumes the generic bilinear form  $J_1 F_1 + J_d F_d$ . A common definition of

efficiency in such cases is given by the ratio between entropy production components  $-J_1 F_1 / J_d F_d$ , describing the partial conversion of one type of energy, expressed in terms of a driving force  $F_d$  with corresponding flux  $J_d$  into another one, characterized by a load force  $F_1$  and flux  $J_1$ . Above relation has been used for describing several systems in nonequilibrium thermodynamics, such as linear stochastic thermodynamics [2, 11, 33], systems in contact presenting a single worksource and heatsource [34], work-to-work transducers [6, 7, 35–37] and others. On the other hand, the class of engines we are investigating can be associated with three thermodynamic forces (two of them are related to  $f_1$ ,  $f_2$  and the third with the difference of temperatures), implying the usage of above ratio as a dubious measure of the system performance for  $T_1 \neq T_2$ . For this reason, we consider a definition of efficiency given by [13, 20, 21]

$$\eta = -\frac{\mathcal{P}}{\bar{W}_1 + \bar{Q}_1 \Theta(-\bar{Q}_1) + \bar{Q}_2 \Theta(-\bar{Q}_2)}, \quad (19)$$

also expressing the partial conversion of a given amount of energy under the form of input heat  $\bar{Q}_1 \Theta(-\bar{Q}_1) + \bar{Q}_2 \Theta(-\bar{Q}_2) < 0$  ( $\Theta(x)$  being the Heaviside function) plus input work  $\bar{W}_1 < 0$  into power output  $\mathcal{P} \equiv \bar{W}_2 \geq 0$ . Eq. (19) reduces to the previous definition for  $\Delta T = T_1 - T_2 = 0$  in which output and input works are related to fluxes as  $\mathcal{P} = -T J_1 F_1$  and  $\bar{W}_1 = -T J_d F_d$  [11, 13, 21, 22]. Since realistic engines operate at finite time, we are going to exploit distinct routes for optimizing the system performance for finite  $\tau$ : by maximizing  $\eta$  and  $\mathcal{P}$  with respect to the  $f_2/f_1$  and  $\alpha$ . Although such maximizations can be directly performed from the expressions for  $\mathcal{P}$  and  $\eta$  from Eqs. (16) and (19), respectively, these expressions are little instructive, due to the complex interplay between  $\alpha$  and  $f_2$ . For this reason, in the next section, we shall present distinct approaches/reasonings for obtaining some maximized quantities with respect to  $\alpha$  (for fixed  $f_1$  and  $f_2$ ) and optimized  $f_2$  (for fixed  $\alpha$  and  $f_1$ ).

### C. Linear approximation for the power output

As stated before, the role of coupling  $\alpha$  and its interplay with  $f_i$ 's and  $T_i$ 's is not evident. In order to obtain some insight about it, the analysis is performed for small  $\alpha$ , in which the average  $\mathcal{P}$  is decomposed in the following way:

$$\mathcal{P} \approx \mathcal{P}_0 + \alpha \mathcal{P}_\alpha. \quad (20)$$

where  $\mathcal{P}_0$  accounts the average power (calculated at the 2-th stage) for the couplingless case. According to Refs. [20, 21],  $\mathcal{P}_0$  can be expressed in terms of Onsager coefficients,  $\mathcal{P}_0 = -T_2(L_{21}f_1 + L_{22}f_2)$ , where each coefficient  $L_{2i}$  is given by

$$\begin{aligned}
L_{22} &= \frac{m}{T_2\tau(e^{\gamma\tau} - 1)} \left[ \int_{\tau/2}^{\tau} h_2(t)e^{-\gamma t} dt \int_{\tau/2}^{\tau} h_2(t')e^{\gamma t'} dt' + (e^{\gamma\tau} - 1) \int_{\tau/2}^{\tau} h_2(t)e^{-\gamma t} \int_{\tau/2}^t h_2(t')e^{\gamma t'} dt' dt \right], \\
L_{21} &= \frac{me^{\gamma\tau}}{T_2\tau(e^{\gamma\tau} - 1)} \int_0^{\tau/2} h_1(t')e^{\gamma t'} dt' \int_{\tau/2}^{\tau} h_2(t)e^{-\gamma t} dt.
\end{aligned} \tag{21}$$

In a similar fashion, expressions for the average work in the

first stage assumes the form  $\bar{W}_{10} = -T_1(L_{11}f_1 + L_{12}f_2)$ , also expressed in terms of Onsager coefficients  $L_{1i}$ 's given by

$$\begin{aligned}
L_{11} &= \frac{m}{T_1\tau(e^{\gamma\tau} - 1)} \left[ (e^{\gamma\tau} - 1) \int_0^{\tau/2} h_1(t)e^{-\gamma t} \int_0^t h_1(t')e^{\gamma t'} dt' dt + \int_0^{\tau/2} h_1(t)e^{-\gamma t} dt \int_0^{\tau/2} h_1(t')e^{\gamma t'} dt' \right], \\
L_{12} &= \frac{m}{T_1\tau(e^{\gamma\tau} - 1)} \int_0^{\tau/2} h_1(t)e^{-\gamma t} dt \int_{\tau/2}^{\tau} h_2(t')e^{\gamma t'} dt'.
\end{aligned} \tag{22}$$

Reciprocal relations for cross coefficients  $L_{12}$  and  $L_{21}$  are derived when drivings are reversed and indices  $1 \leftrightarrow 2$  exchanged [21, 38]. The linear contribution  $\mathcal{P}_\alpha$  can also be expressed in the following generic form:

$$\mathcal{P}_\alpha = T_2 f_2 (\tilde{L}_{222} f_2^2 + \tilde{L}_{211} f_1^2 + \tilde{L}_{221} f_2 f_1), \tag{23}$$

where general expressions for coefficients  $\tilde{L}_{2jk}$ 's are listed in Appendix A and B for generic and constant and linear drivings, respectively. However, in contrast to Onsager ones, above coefficients  $\tilde{L}_{ijk}$ 's do not necessarily satisfy the stan-

dard reciprocal relations [20, 21, 38]. Analogously to  $\mathcal{P}_\alpha$ , the linear contribution for  $\bar{W}_{1\alpha}$  can also be expressed in following form given by  $\bar{W}_{1\alpha} = T_1 f_1 (\tilde{L}_{111} f_1^2 + \tilde{L}_{221} f_2^2 + \tilde{L}_{112} f_2 f_1)$ , whose coefficients  $\tilde{L}_{1jk}$ 's are also listed in Appendix A. From Eq. (23), the optimal force  $f_{2P}$  providing maximum power  $\mathcal{P}_P$  are straightforwardly obtained and given by

$$f_{2P} = \frac{-(L_{22} + \alpha f_1 \tilde{L}_{221})}{3\alpha \tilde{L}_{222}} \left[ 1 - \sqrt{1 - \frac{3\alpha f_1 \tilde{L}_{222} (L_{21} + \alpha f_1 \tilde{L}_{221})}{(L_{22} + \alpha f_1 \tilde{L}_{221})^2}} \right], \tag{24}$$

and

$$\frac{\mathcal{P}_P}{T_2} = \frac{2(\alpha f_1 \tilde{L}_{221} + L_{22})^2 (\alpha f_1 \tilde{L}_{221} + L_{22} - \mathcal{A}) - 3\alpha f_1 \tilde{L}_{222} (\alpha f_1 \tilde{L}_{211} + L_{21}) (3\alpha f_1 \tilde{L}_{221} + 3L_{22} - 2\mathcal{A})}{27\alpha^2 \tilde{L}_{222}^2},$$

respectively, where  $\mathcal{A}$  reads  $\mathcal{A} = \sqrt{(\alpha f_1 \tilde{L}_{221} + L_{22})^2 - 3\alpha f_1 \tilde{L}_{222} (\alpha f_1 \tilde{L}_{211} + L_{21})}$ . Note that one recovers the expression  $2f_{2P} = -L_{21}/L_{22}$  and  $\mathcal{P}_P = T_2 L_{21}^2 f_1 / 4L_{22}$  as  $\alpha = 0$ .

#### D. Approximate descriptions for maximum efficiencies

Since the average heat components  $\bar{Q}_{1f}$  and  $\bar{Q}_{2f}$  are always positive, the system solely will receive heat from the  $i$ -th thermal bath from a temperature difference  $\Delta T$  in which  $\bar{Q}_i = \bar{Q}_{if} + \bar{Q}_{f_1, f_2, T_i} < 0$ . Giving that above condition is always fulfilled for large  $\Delta T$  and by the fact that the power output  $\mathcal{P}$  does not depend on the temperatures, the efficiency of

thermal engines for  $\alpha = 0$  always decreases when compared to its corresponding work-to-work converter  $\eta_{w \rightarrow w} = -\mathcal{P}/\bar{W}_1$ . However, a coupling between drivings and velocities makes possible to (properly) adjust the coupling ensuring a maximum efficiency. Despite the complex interplay between  $\alpha$  and  $f_1, f_2$  leads to very cumbersome expressions for maximized quantities (above all the efficiency), it is possible to predict optimized expressions for efficiency by means of two simple reasonings, as described as follows: The first analysis can be performed in the regime of small  $\alpha$ , in which, in similarity to the expansion for  $\mathcal{P}$  and  $\bar{W}_1$ , one assumes the following expansions for  $\bar{Q}_1$  and  $\bar{Q}_2$ :

$$\bar{Q}_1 = \bar{Q}_{10} + \alpha \bar{Q}_{1\alpha}, \quad \bar{Q}_2 = \bar{Q}_{20} + \alpha \bar{Q}_{2\alpha}, \tag{25}$$

By inserting above expressions in Eq. (19) and considering up to the linear term, the efficiency is given by  $\eta \approx \eta_0 + \alpha\eta_\alpha$ , where  $\eta_0$  and  $\eta_\alpha$  read:

$$\eta_0 = -\frac{\mathcal{P}_0}{\bar{W}_{10} + \bar{Q}_{10}\Theta(-\bar{Q}_{10}) + \bar{Q}_{20}\Theta(-\bar{Q}_{20})}, \quad (26)$$

and

$$\eta_\alpha = \frac{\mathcal{P}_\alpha - \eta_0 \left[ \bar{W}_{1\alpha} + \bar{Q}_{1\alpha}\Theta(-\bar{Q}_{1\alpha}) + \bar{Q}_{2\alpha}\Theta(-\bar{Q}_{2\alpha}) \right]}{\bar{W}_{10} + \bar{Q}_{10}\Theta(-\bar{Q}_{10}) + \bar{Q}_{20}\Theta(-\bar{Q}_{20})}, \quad (27)$$

respectively. Note that  $\eta_0$  solely depends on 0-th order quantities (as expected), whereas  $\eta_\alpha$  depends on  $\eta_0$ ,  $\bar{W}_{i\alpha}$ 's and  $\bar{Q}_{i\alpha}$ 's. Maximization of  $\eta$  with respect to  $f_2$ , providing  $f_{2mE}$ , can be calculated from Eqs. (26) and (27).

Contrariwise, for the case in which above approximation for small  $\alpha$  is not valid, maximization of efficiency can be carried out by means of a simple argument, as described as follows: Let us consider the case in which the average heat component  $\bar{Q}_{f_1, f_2, T_i}$  dominates over  $\bar{Q}_{if}$  ( $|\bar{Q}_{f_1, f_2, T_i}| \gg \bar{Q}_{if}$ ). Although this is verified for sufficient large  $|\Delta T|$  and fixed  $f_1, f_2$ , such condition can be fulfilled for other interplay among parameters. For situations in which the power output monotonically increases (this is promptly verified for the drivings considered here) upon  $\alpha$  is varied, the efficiency can be enhanced by searching for the optimal coupling  $\alpha_E$ , in which  $\bar{Q}_{if} + \bar{Q}_{f_1, f_2, T_i} \approx \bar{Q}_{f_1, f_2, T_i} = 0$ :

$$\alpha_E = \frac{T_1 - T_2}{f_1 T_2 - f_2 T_1}. \quad (28)$$

Note that above approximate relation is general and expresses the interplay among driving strengths and temperatures and approaches to 0 as  $\Delta T \rightarrow 0$  for finite  $f_1 - f_2$ , showing that forces proportional to the velocity can increase the efficiency for suited choice of temperatures and forces. The corresponding maximum efficiency  $\eta_{\alpha_E, f_1, f_2, \Delta T}$  reduces to the work-to-work converter expression given by

$$\bar{\eta}_{f_2, f_1, \Delta T} = -\frac{\mathcal{P}_E^*}{\bar{W}_{1E}^*}, \quad (29)$$

with  $\mathcal{P}_E^* = \mathcal{P}(f_1, f_2, \Delta T, \tau)$  and  $\bar{W}_{1E}^* = \bar{W}_1(f_1, f_2, \Delta T, \tau)$  denoting the  $\mathcal{P}$  and  $\bar{W}_1$  evaluated at  $\alpha = \alpha_E$ , respectively. Note that Eq. (29) solely depends on  $f_1, f_2, \tau$  and  $\Delta T$ . The efficiency can also be maximized with respect to  $f_2$  (for fixed  $\Delta T$ ) or  $\Delta T$  (for fixed  $f_2$ ). Although it can be directly carried out by a simultaneous maximization of Eq. (19), an approximate expression for the simultaneous maximum efficiency  $\eta_{f_1, \theta}^*$  ( $\theta = f_2$  or  $\Delta T$ ) is obtained by searching for  $f_2$  or  $\Delta T$  that maximizes Eq. (29):

$$\eta_{f_1, \theta}^* = -\frac{\mathcal{P}_{mE}^*}{\bar{W}_{1mE}^*}, \quad (30)$$

where  $\mathcal{P}_{mE}^* = \mathcal{P}(f_1, \theta_E, \tau)$  and  $\bar{W}_{1mE}^* = \bar{W}_1(f_1, \theta_E, \tau)$  denoting the  $\mathcal{P}$  and  $\bar{W}_1$  evaluated at  $\alpha = \alpha_E$  and  $f_2 = f_{2E}$  ( $\theta = \Delta T$ ) or  $\Delta T = \Delta T_E$  ( $\theta = f_2$ ) respectively.

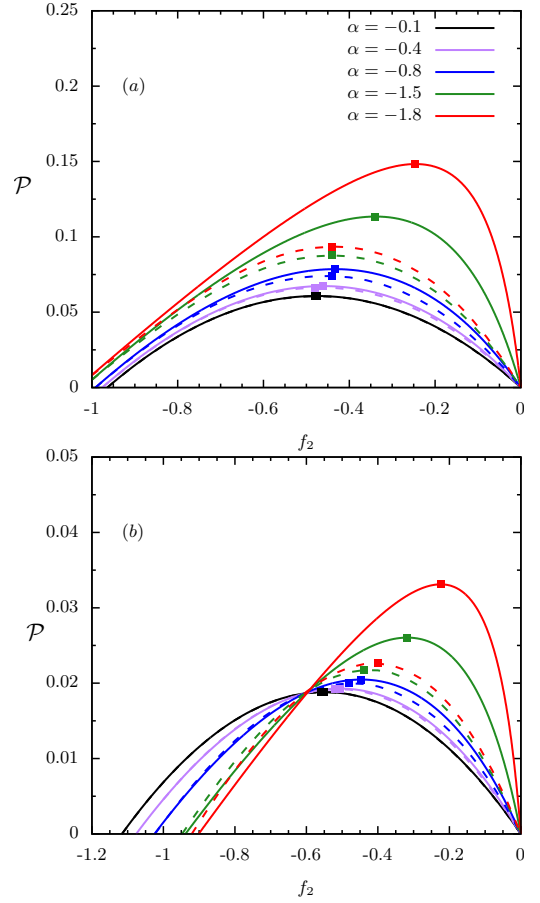


FIG. 1. For constant (a) and linear (b) drivings, the depiction of power output  $\mathcal{P}$  (continuous) and those from a linear analysis (dashed), where squares correspond to  $f_{2p}$ 's ensuring maximum power  $\mathcal{P}_p$ 's. Parameters:  $m = \tau = \gamma = 1, f_1 = 1$ .

### III. RESULTS

In all cases, analysis will be carried out for constant and linear drivings and the following parameters choices  $m = \tau = \gamma = f_1 = 1$ . Expressions for Onsager and coefficients from the linear analysis are listed in Appendix B. In the first round of analysis, the influence of  $\alpha$  over the power output  $\mathcal{P}$  and efficiency  $\eta$  are exemplified for some sort of parameters, as depicted in Figs. 1-2 for constant and linear drivings.  $\mathcal{P}$  (Fig. 1) monotonically increases with the absolute value of  $\alpha$ , having this feature captured by the linear analysis for small  $\alpha$ . In other words, apart from the increase of power as the absolute value of  $\alpha$  increases, there is no optimal coupling leading to maximum power, implying its maximization solely with respect to the force  $f_2$  in which  $\mathcal{P}_p$ .

The influence of  $\alpha$  over the efficiency is more revealing and exemplified in Fig. 2 for two representative temperature differences:  $\Delta T = 0.25$  ( $T_1 > T_2$ ) and  $\Delta T = -0.25$  ( $T_1 < T_2$ ). In both cases, efficiencies are rather small when  $\alpha = 0$  (couplingless case) and an optimal coupling between driving and velocities ensures substantial increases (see e.g. dashed lines). Also, efficiency curves behave quite differently with respect to

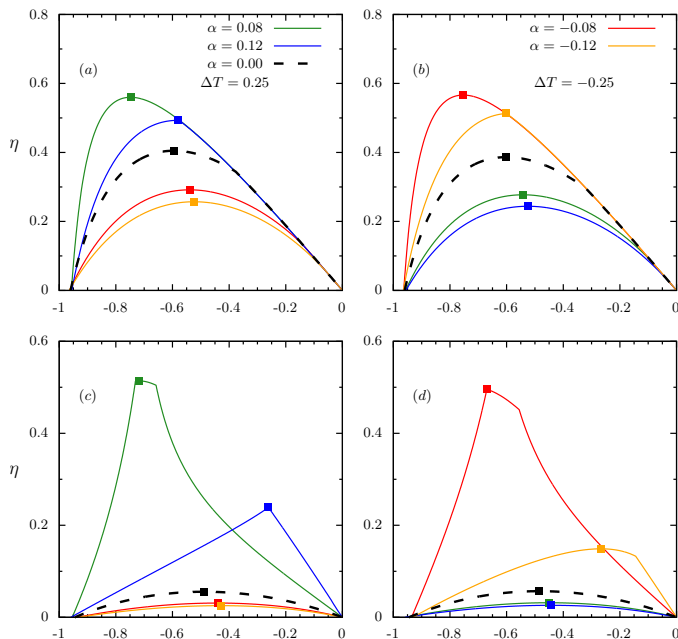


FIG. 2. For constant drivings, the depiction of efficiency  $\eta$  for representative values of  $\alpha$  and distinct  $\Delta T$ 's. In (a)/(c) and (b)/(d),  $T_1$  reads  $T_1 = 2.0$  and  $T_1 = 1.75$ , respectively. Squares denote the associate maximum efficiencies (with respect to the  $f_2$ ). Parameters:  $m = \tau = \gamma = f_2 = 1$ .

$\alpha = 0$ . This is due to the influence of parameters (mainly  $f_2$ ,  $\alpha$  and  $\Delta T$ ) on the average works and on the amount of a received heat [see e.g. denominator from Eq. (19)] and it is more significant for linear drivings (see e.g. Fig. 2), where efficiencies are just smaller [20, 22]. Thus, whenever  $\mathcal{P}$  ( $\bar{W}_1^*$ ) always increases with the absolute value of  $\alpha$ , there is an optimal coupling  $\alpha_E$  controlling/decreases the amount of "wasted" average heat. In particular, the optimal coupling  $\alpha_E$  is positive and negative for  $T_1 > T_2$  and  $T_1 < T_2$ , respectively.

For above set of parameters, Figs. 3-5 provides a global overview about the role of  $\alpha$  by depicting heat maps (phase diagrams) for  $\mathcal{P}$  and  $\eta$  for linear and constant drivings. As in Fig. 1,  $\mathcal{P}$  monotonically increases with the coupling and providing, for all values of  $\alpha$ , optimal  $f_{2P}$ 's ensuring maximal  $\mathcal{P}_P$  (red lines). Contrasting to the power output, in which a simultaneous maximization of power is not possible, efficiencies phase diagrams (Figs. 4 and 5) exhibit a central region in which efficiency can be simultaneously maximized. Maximum lines behave differently, reflecting the distinct dependence between  $\eta$  with  $\alpha$  and  $f_2$ . They meet at the vicinity of global maximum. Approximate curves (dotted lines), obtained from Eq. (28), approach to exact ones (dashed) as  $\Delta T$  is raised. They are always closer to each other for linear than constant drivings. Such findings are complemented in Fig. 6, consistent with reliability by neglecting  $\underline{Q}_{if}$  as  $|\Delta T|$  raises.

Fig. 7 shows maximum efficiencies  $\bar{\eta}_{f_2, f_1, \Delta T}$  and  $\eta_{f_1, \Delta T}^*$ , obtained from direct maximization and by comparing expressions from Eqs. (29) and (30), respectively. Note the excellent agreement between exact and approximate expressions (de-

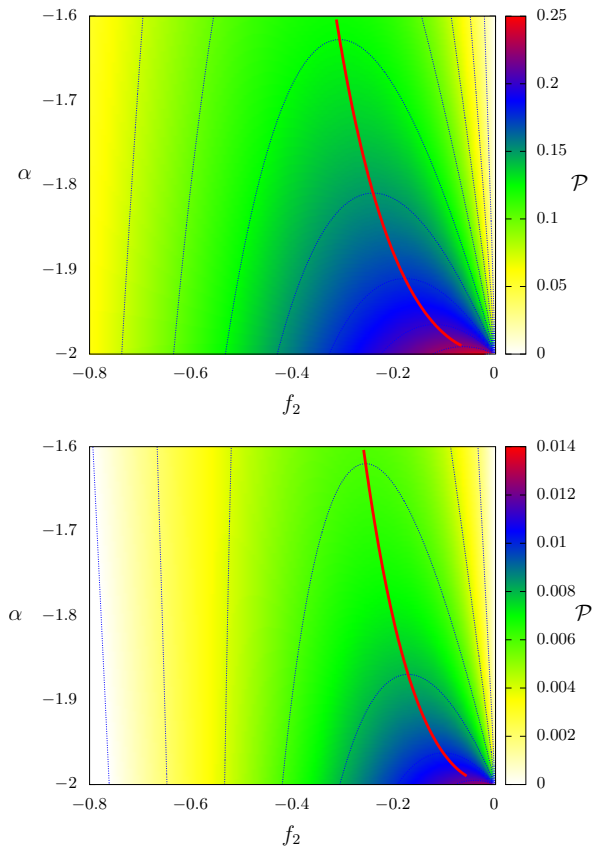


FIG. 3. For constant (top) and linear (bottom) drivings, the depiction of power output  $\mathcal{P}$  in the plane  $(f_2, \alpha)$ . For each  $\alpha$ , red lines denote the locus  $(f_{2P}, \mathcal{P}_P)$  of maximum  $\mathcal{P}$  with respect to  $f_2$ . Parameters:  $m = \tau = \gamma = 1, f_1 = 1$ .

viations among curves are almost imperceptible), reinforcing the search for optimal parameters for maximum efficiencies. At the vicinity of optimal couplings, they are substantially larger than  $\bar{\eta}_{f_1, \Delta T} = 0.4049/0.0555$  and  $0.1822/0.0151$  (see e.g. Fig 2), obtained for the couplingless constant/linear cases for  $\Delta T = 0.25$  and 1, respectively.

Finally, Fig. 8 illustrates a phase diagram  $\Delta T$  versus  $f_2$  for constant drivings. Note that the increase of  $\Delta T$  together an optimal choice of  $f_2$  increases the efficiency. Thus, the coupling may also provide a suitable choice of temperature difference in order to enhance the efficiency or furnish a desirable value for it.

#### IV. CONCLUSIONS

Collisional Brownian engines constitute a very simple class of machines having thermodynamic properties exactly obtained irrespective the driving, temperature of thermal baths and the duration of each stage. Notwithstanding, its performance can decrease substantially depending on the way it is projected (period, duration of stage, temperature of baths and drivings). In order to address possible improvements in such class of systems, the influence of velocity driving component

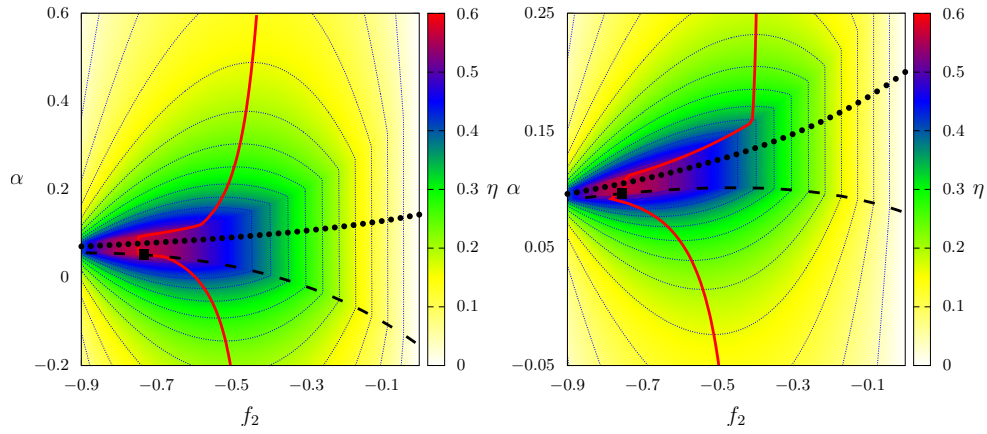


FIG. 4. For the same parameters of Fig. 2, the efficiency phase diagrams  $\alpha$  versus  $f_2$  for  $\Delta T = 0.25$  (left) and  $-0.25$  (right). Continuous, dashed and dotted lines correspond to the maximization with respect to  $f_2$  (fixed  $\alpha$ ),  $\alpha$  (fixed  $f_2$ ) and approximate [from Eq. (28)], respectively. "Squares" denote the simultaneous maximization with respect to  $\alpha$  and  $f_2$ .

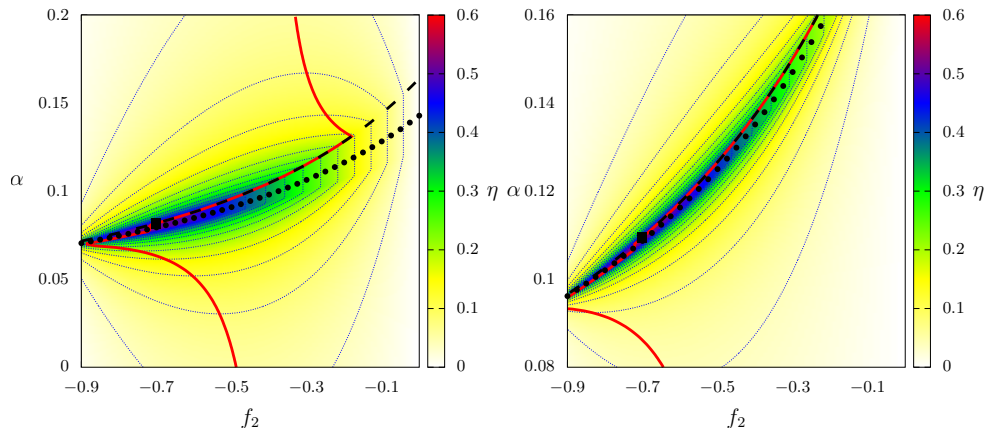


FIG. 5. For the same parameters of Fig. 2, the efficiency phase diagrams  $\alpha$  versus  $f_2$  for  $\Delta T = 0.25$  (left) and  $-0.25$  (right). Continuous, dashed and dotted lines correspond to the maximization with respect to  $f_2$  (fixed  $\alpha$ ),  $\alpha$  (fixed  $f_2$ ) and approximate [from Eq. (28)], respectively. "Squares" denote the simultaneous maximization with respect to  $\alpha$  and  $f_2$ .

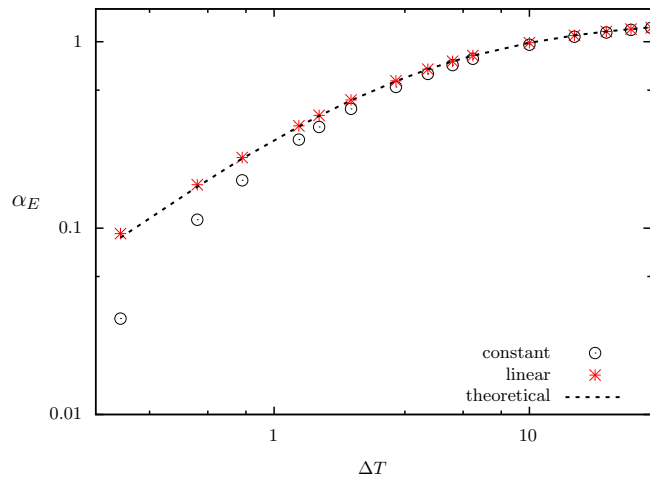


FIG. 6. Comparison among logarithm plots of  $\alpha_E$  obtained from Eq.(28) (dashed lines) and from direct maximization of Eq. (19) for constant (circles) and linear (stars) drivings. Parameters:  $T_2 = 1.5$ ,  $m = \tau = \gamma = 1$ ,  $f_1 = 1$  and  $f_2 = -0.75$ .

was introduced and analyzed from the framework of stochastic thermodynamics. Results for constant and linear drivings reveal that it can be conveniently considered in order to optimize efficiency, even for large temperature differences between thermal reservoirs, where the couplingless engine operates very inefficiently. Distinct maximization routes were considered and substantial improvements can be gained. Despite the results, the absence of a simultaneous maximization for the power output for constant and linear drivings, we underscore a reliable choice of coupling  $\alpha$  can be taken for ensuring a compromise between the power output and efficiency.

As potential perspectives of the present work, it might be interesting to address other kinds of maximizations, such as by holding the dissipation fixed as well as the influence of the coupling in such cases. Finally, it might also be remarkable to extend the collisional approach for massive Brownian particles in order to compare their performances.

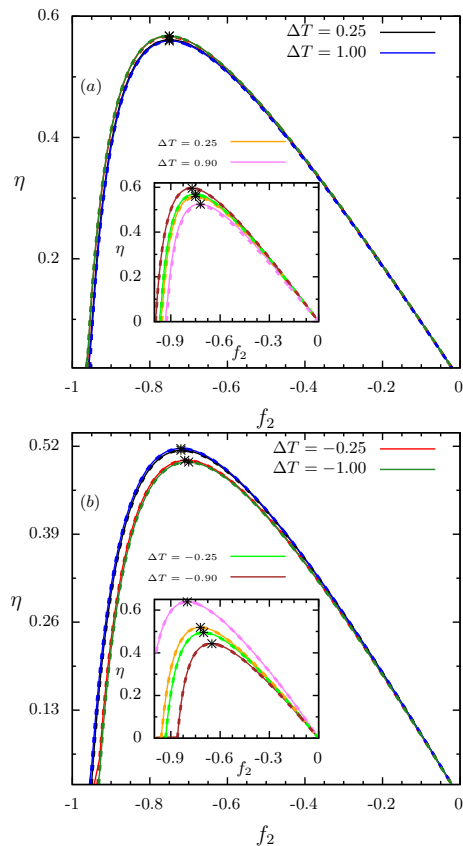


FIG. 7. For the same parameters from Figs. 4 and 5, main panels show efficiency maxima  $\bar{\eta}_{f_2, f_1, \Delta T}$  versus  $f_2$  for distinct  $\Delta T$ 's for constant and linear drivings, respectively. Inset: Results for the same  $\Delta T$  but for  $T_1 = 0.1, 1, 1$  and  $1.25$ , respectively. Stars denote the prediction from Eq. (30) for maximized efficiencies  $\bar{\eta}_{f_2, f_1, \Delta T}$ 's with respect to  $\alpha$  and  $f_2$ . Continuous and dashed lines correspond to exact and efficiencies evaluated from Eq. (29), respectively.

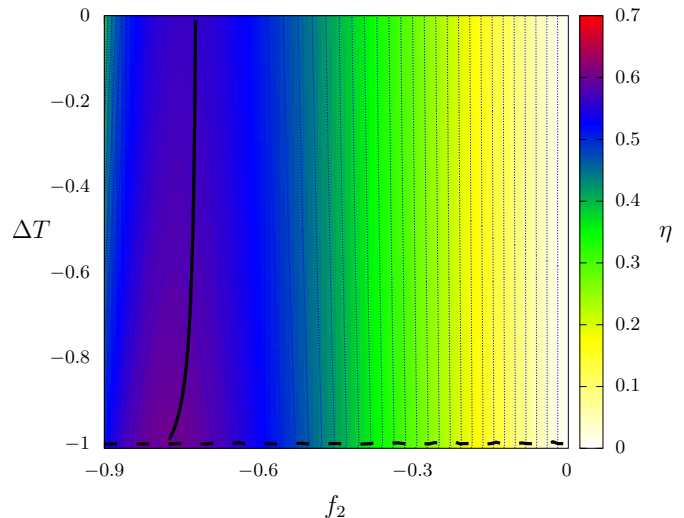


FIG. 8. For constant drivings, the efficiency phase diagram  $\Delta T$  versus  $f_2$ . Continuous and dashed lines denote the maximization respect to the  $f_2$  and  $\Delta T$ , respectively.

## V. ACKNOWLEDGMENT

I. N. Mamede and C. E. F. acknowledge the financial support from FAPESP under grants 2021/12551-8 and 2021/03372-2, respectively. The financial supports from CNPq and CAPES are also acknowledged.

- 
- [1] H. B. Callen, John Wiley & Sons, New York (1960).
  - [2] C. Van den Broeck, *Phys. Rev. Lett.* **95**, 190602 (2005).
  - [3] U. Seifert, *Rep. Prog. Phys.* **75**, 126001 (2012).
  - [4] S. Rana, P. Pal, A. Saha, and A. Jayannavar, *Physical review E* **90**, 042146 (2014).
  - [5] I. A. Martínez, É. Roldán, L. Dinis, D. Petrov, J. M. Parrondo, and R. A. Rica, *Nature physics* **12**, 67 (2016).
  - [6] S. Liepelt and R. Lipowsky, *Phys. Rev. Lett.* **98**, 258102 (2007).
  - [7] S. Liepelt and R. Lipowsky, *Phys. Rev. E* **79**, 011917 (2009).
  - [8] J. Seader, (1982).
  - [9] M. Esposito, R. Kawai, K. Lindenberg, and C. Van den Broeck, *Phys. Rev. E* **81**, 041106 (2010).
  - [10] J. A. Albay, Z.-Y. Zhou, C.-H. Chang, and Y. Jun, *Scientific reports* **11**, 1 (2021).
  - [11] K. Proesmans, Y. Dreher, M. Gavrilov, J. Bechhoefer, and C. Van den Broeck, *Physical Review X* **6**, 041010 (2016).
  - [12] N. Golubeva and A. Imparato, *Phys. Rev. Lett.* **109**, 190602 (2012).
  - [13] I. N. Mamede, P. E. Harunari, B. A. N. Akasaki, K. Proesmans, and C. E. Fiore, *Phys. Rev. E* **105**, 024106 (2022).
  - [14] Y. Jun, M. Gavrilov, and J. Bechhoefer, *Physical review letters* **113**, 190601 (2014).
  - [15] C. H. Bennett, *International Journal of Theoretical Physics* **21**, 905 (1982).
  - [16] K. Maruyama, F. Nori, and V. Vedral, *Reviews of Modern Physics* **81**, 1 (2009).
  - [17] T. Sagawa, *Journal of Statistical Mechanics: Theory and Experiment* **2014**, P03025 (2014).
  - [18] J. M. Parrondo, J. M. Horowitz, and T. Sagawa, *Nature physics* **11**, 131 (2015).
  - [19] P. E. Harunari, F. S. Filho, C. E. Fiore, and A. Rosas, *Phys. Rev. Research* **3**, 023194 (2021).
  - [20] C. E. F. Noa, A. L. L. Stable, W. G. C. Oropesa, A. Rosas, and C. E. Fiore, *Phys. Rev. Research* **3**, 043152 (2021).
  - [21] F. S. Filho, B. A. Akasaki, C. E. F. Noa, B. Cleuren, C. E. Fiore, *et al.*, arXiv preprint arXiv:2206.05819 (2022).
  - [22] C. F. Noa, W. G. Oropesa, and C. Fiore, *Physical Review Research* **2**, 043016 (2020).
  - [23] C. Ganguly and D. Chaudhuri, *Phys. Rev. E* **88**, 032102 (2013).
  - [24] F. Schweitzer, W. Ebeling, and B. Tilch, *Phys. Rev. Lett.* **80**, 5044 (1998).



- [25] S. Dago, J. Pereda, S. Ciliberto, and L. Bellon, *Journal of Statistical Mechanics: Theory and Experiment* **2022**, 053209 (2022).
- [26] J. R. Howse, R. A. Jones, A. J. Ryan, T. Gough, R. Vafabakhsh, and R. Golestanian, *Physical review letters* **99**, 048102 (2007).
- [27] W. F. Paxton, K. C. Kistler, C. C. Olmeda, A. Sen, S. K. St. Angelo, Y. Cao, T. E. Mallouk, P. E. Lammert, and V. H. Crespi, *Journal of the American Chemical Society* **126**, 13424 (2004).
- [28] F. Schweitzer and J. D. Farmer, *Brownian agents and active particles: collective dynamics in the natural and social sciences*, Vol. 1 (Springer, 2003).
- [29] T. Tomé and M. J. De Oliveira, *Stochastic dynamics and irreversibility* (Springer, 2015).
- [30] T. Tomé and M. J. de Oliveira, *Physical Review E* **82**, 021120 (2010).
- [31] T. Tomé and M. J. de Oliveira, *Physical review E* **91**, 042140 (2015).
- [32] M. Esposito and C. Van den Broeck, *Physical Review E* **82**, 011143 (2010).
- [33] K. Proesmans, C. Driesen, B. Cleuren, and C. Van den Broeck, *Physical review E* **92**, 032105 (2015).
- [34] H. Vroylandt, M. Esposito, and G. Verley, *EPL (Europhysics Letters)* **120**, 30009 (2017).
- [35] T. Herpich, J. Thingna, and M. Esposito, *Phys. Rev. X* **8**, 031056 (2018).
- [36] T. Herpich and M. Esposito, *Phys. Rev. E* **99**, 022135 (2019).
- [37] D. M. Busiello and C. Fiore, arXiv preprint arXiv:2205.00294 (2022).
- [38] A. Rosas, C. Van den Broeck, and K. Lindenberg, *Phys. Rev. E* **97**, 062103 (2018).

## Appendix

### A. Coefficients of the linear approximation for small couplings

Below, we list the expressions for coefficients  $\tilde{L}_{ijk}$ 's from the linear expansion of  $\mathcal{P}$  and  $\bar{W}_1$  for generic drivings  $h_1(t)$  and  $h_2(t)$ :

$$\tilde{L}_{111} = \frac{\alpha}{2\tau T_1} \int_0^{\frac{\tau}{2}} e^{-\gamma t} \left[ \frac{\mathcal{F}_1\left(\frac{\tau}{2}, 0\right) (e^{\gamma\tau}(2t + \tau) - 2t)}{(e^{\gamma\tau} - 1)^2} + 2t\mathcal{F}_1(t, 0) \right] dt, \quad (\text{A1})$$

$$\tilde{L}_{112} = \frac{\alpha e^{\frac{3\gamma\tau}{4}} \sinh\left(\frac{\gamma\tau}{4}\right)}{\gamma^2 \tau (e^{\gamma\tau} - 1)^2 T_1} \left[ \gamma\tau \mathcal{F}_1\left(\frac{\tau}{2}, 0\right) + \mathcal{F}_2(\tau, 0) \left( 4 \sinh\left(\frac{\gamma\tau}{2}\right) - \gamma\tau \right) \right], \quad (\text{A2})$$

$$\tilde{L}_{122} = \frac{\alpha e^{\gamma\tau} (e^{\frac{\gamma\tau}{2}} - 1) \mathcal{F}_2(\tau, 0)}{2\gamma (e^{\gamma\tau} - 1)^2 T_1}, \quad (\text{A3})$$

$$\tilde{L}_{222} = \frac{\alpha}{2\tau (e^{\gamma\tau} - 1)^2 T_2} \int_{\frac{\tau}{2}}^{\tau} e^{\frac{1}{2}\gamma(\tau-2t)} \left[ \mathcal{F}_2(\tau, 0) (2t (e^{\gamma\tau} - 1) + \tau) - (e^{\gamma\tau} - 1)^2 (\tau - 2t) \mathcal{F}_2(t, 0) \right] dt, \quad (\text{A4})$$

$$\tilde{L}_{221} = \frac{\alpha \left[ \coth\left(\frac{\gamma\tau}{4}\right) - 1 \right] \operatorname{sech}^2\left(\frac{\gamma\tau}{4}\right) \left[ \mathcal{F}_1\left(\frac{\tau}{2}, 0\right) \left( 4 \sinh\left(\frac{\gamma\tau}{2}\right) - \gamma\tau \right) + \gamma\tau \mathcal{F}_2(\tau, 0) \right]}{16\gamma^2 \tau T_2}, \quad (\text{A5})$$

and

$$\tilde{L}_{211} = \frac{\alpha e^{\gamma\tau} (e^{\frac{\gamma\tau}{2}} - 1) \mathcal{F}_1\left(\frac{\tau}{2}, 0\right)}{2\gamma (e^{\gamma\tau} - 1)^2 T_2}. \quad (\text{A6})$$

### B. Coefficients of the linear approximation for constant and linear drivings

As stated in the main text, by inserting explicit expressions for drivings  $h_1(t)$  and  $h_2(t)$ , Onsager coefficients  $L_{ij}$ 's and  $\tilde{L}_{ijk}$ 's can be straightforwardly obtained from Eqs. (21)-(22) and (A1)-(A6), respectively. For constant drivings, we arrive at the following expressions:

$$T_1 L_{11} = T_2 L_{22} = \frac{1}{\gamma} \left( \frac{1}{2} - \frac{\tanh\left(\frac{\gamma\tau}{4}\right)}{\gamma\tau} \right), \quad T_1 L_{12} = T_2 L_{21} = \frac{1}{\gamma^2 \tau} \tanh\left(\frac{\gamma\tau}{4}\right) \quad (\text{A7})$$

for Onsager ones and

$$T_1 \tilde{L}_{111} = T_2 \tilde{L}_{222} = \frac{\gamma\tau \left( \operatorname{sech}^2\left(\frac{\gamma\tau}{4}\right) + 4 \right) - 16 \tanh\left(\frac{\gamma\tau}{4}\right)}{8\gamma^3\tau} \quad (\text{A8})$$

$$T_1 \tilde{L}_{122} = T_2 \tilde{L}_{211} = \frac{\left( 4 \sinh\left(\frac{\gamma\tau}{2}\right) - \gamma\tau \right) \operatorname{sech}^2\left(\frac{\gamma\tau}{4}\right)}{8\gamma^3\tau} \quad (\text{A9})$$

$$T_1 \tilde{L}_{112} = T_2 \tilde{L}_{221} = \frac{\tanh\left(\frac{\gamma\tau}{4}\right)}{\gamma^3\tau} \quad (\text{A10})$$

for the linear contribution of  $\alpha$ . Similarly, for linear drivings, their expressions are listed below:

$$T_1 L_{111} = T_2 L_{222} = \frac{\gamma\tau(\gamma\tau - 2) + 2(4 - \gamma\tau) \tanh\left(\frac{\gamma\tau}{4}\right)}{8\gamma^3\tau}, \quad T_1 L_{112} = T_2 L_{211} = \frac{(\gamma\tau - 4) \tanh\left(\frac{\gamma\tau}{4}\right) + \gamma\tau}{4\gamma^3\tau} \quad (\text{A11})$$

for Onsager ones and

$$T_1 \tilde{L}_{111} = \frac{-\gamma^2\tau^2 + e^{\frac{3\gamma\tau}{2}} [\gamma\tau(\gamma\tau - 8) + 24] + e^{\gamma\tau} [\gamma\tau(\gamma\tau - 4) - 24] - 3e^{\frac{\gamma\tau}{2}} [\gamma\tau(\gamma\tau - 4) + 8] + 24}{8\gamma^4\tau \left( e^{\frac{\gamma\tau}{2}} - 1 \right) \left( e^{\frac{\gamma\tau}{2}} + 1 \right)^2}, \quad (\text{A12})$$

$$T_1 \tilde{L}_{122} = T_2 \tilde{L}_{211} = \frac{\left( e^{\frac{\gamma\tau}{2}} - 1 \right) \left[ 2e^{\frac{3\gamma\tau}{2}} (\gamma\tau - 4) + 2e^{\gamma\tau} (\gamma\tau + 4) + e^{\frac{\gamma\tau}{2}} [\gamma\tau(\gamma\tau - 4) + 8] - 8 \right]}{4\gamma^4\tau \left( e^{\gamma\tau} - 1 \right)^2} \quad (\text{A13})$$

and

$$T_1 \tilde{L}_{112} = T_2 \tilde{L}_{221} = \frac{\left[ \gamma\tau + (\gamma\tau - 4) \tanh\left(\frac{\gamma\tau}{4}\right) \right]}{4\gamma^4\tau} \quad (\text{A14})$$

for the linear contribution in  $\alpha$ .